An inside look at how AM commercial aluminum alloys are made possible using RAM technology


A6061-RAM2 heat sink - glass bead blasted.

Six months ago, Elementum 3D released the highly desirable aluminum 6061 alloy to the public, proving that commercial alloys are suitable for production of high quality components with current additive processes. As of 2017, only about 12 metal alloys were widely used for laser powder bed fusion (L-PBF) AM processes. The limited selection of proven materials for additive manufacturing (AM) restricts its strategic and economic advantage over traditional manufacturing techniques for many applications. High strength aluminum grades have been especially problematic for fusion AM processes. Many desirable aluminum alloys including 2024, 6061, and 7075 suffer from solidification issues including hot tearing during L-PBF AM that results in parts with very poor mechanical properties.

Elementum 3D has utilized innovative reactive additive manufacturing (RAM) technology to introduce new commercial aluminum alloys and high-performance metal matrix composites for use with existing additive manufacturing equipment. RAM utilizes exothermic chemical reactions to synthesize product materials in situ during the additive fusion process. The RAM process can be used to produce a wide range of materials but is especially well suited for producing ceramic reinforced metal matrix composites (MMCs) by reactively synthesizing ceramic reinforcements. The process can synthesize sub-micron ceramic reinforcements from larger AM feedstock powders that are optimized for process flow and spreadability.
The sub-micron reinforcements also serve as nucleants during alloy solidification to produce favorable fine-grained equiaxed aluminum microstructures. By nucleating a fine equiaxed microstructure, the process overcomes printability problems from hot tearing that have plagued many aluminum alloys. With small fractions of synthesized ceramic, alloys like 2024 and 6061 become printable and behave comparable to their wrought counterparts. Increasing the ceramic fraction results in a tailorable increase in strength, modulus, wear resistance, and elevated temperature performance, while decreasing the coefficient of thermal expansion and ductility.

The chemical energy released by the RAM process assists with processing speed by reducing the amount of laser or other directed energy input required. In addition, high melting temperature ceramic reinforcements can be formed from lower melting temperature precursors to enable energy efficient formation of near full theoretical density composites.

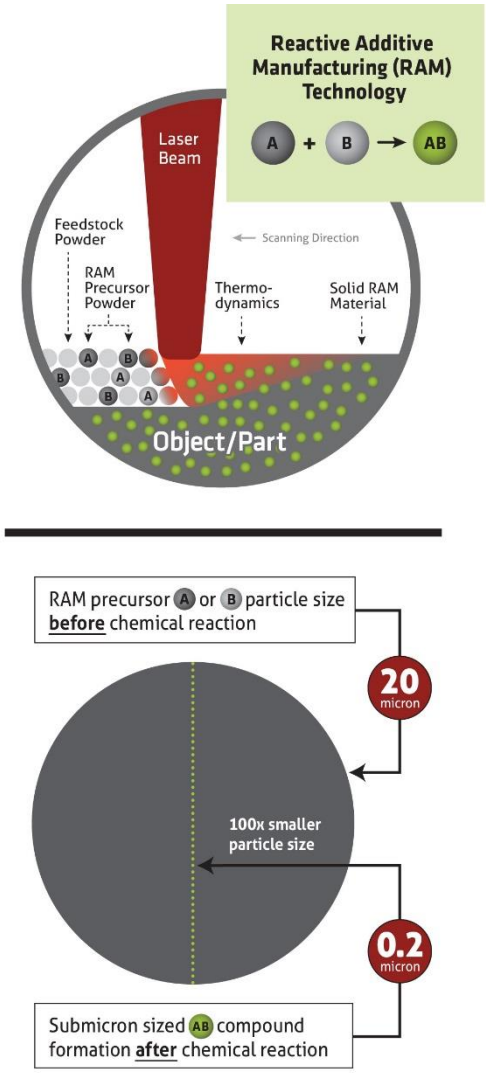

The RAM process uses in-situ chemical reactions during the additive manufacturing process to form beneficial nano or sub-micron scale product phases. The sub-micron products serve as nucleants during alloy solidification to produce favorable fine-grained equiaxed microstructures. The RAM process eliminates problems from residual stresses and hot tearing that have plagued other additive processes.

Adiabatic reaction temperature calculations utilize an iterative approach to solving the energy balance integral shown in Equation (1) using tabulated thermodynamic data such as from NIST-JANNAF for temperature dependent heat capacities, latent heats, and heats of formation. The thermodynamic calculations assist design of the reaction system and in determining the laser energy requirements. The adiabatic combustion temperature, $T_{ad}(298)$, can be calculated with an iterative approach using tabulated thermodynamic data such as from NIST-JANNAF with the energy balance shown in Equation 1.

$$\Delta H(298) + \int_{298}^{T_{ad}(298)} \sum n_j C_p(P_j) dT + \sum_{298-T_{ad}(298)} n_j L(P_j) = 0 \qquad (1)$$

Where $\Delta H(298)$ is the reaction enthalpy at 298 K, n_j is the number of moles of species j, $C_p(P_j)$ is the constant pressure heat capacity of the product species, and $L(P_j)$ is the transformation enthalpy of the products if they undergo a phase change.

An example RAM stoichiometric equation is shown in Equation (2) where A and B represent the reactant species and C represents the product species with Al representing the matrix alloy. The fraction of the metal matrix phase can be adjusted by modifying the value of x in Equation (2).

$$A + B + xAl \rightarrow C + xAl \qquad (2)$$

The fraction of the metal matrix phase can be adjusted by modifying the value of x in Equation (2).

Results

Al2024 was evaluated for L-PBF AM by producing cubes and tensile bars for evaluation. The Al2024 components displayed extremely poor mechanical properties and fracture surfaces exhibited large columnar grains as shown in Figure 1 with intergranular cracking evident as shown in Figure 2. These results are typical for many additively manufactured wrought aluminum alloys including many 2000, 5000, 6000, and 7000 series alloys.

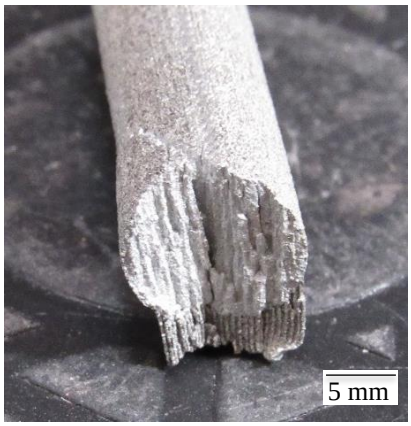

Figure 1: Macroscopic image of Al2024 without RAM additions showing columnar grains.

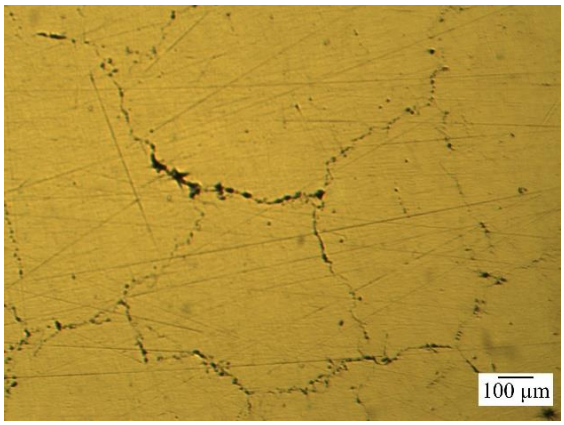

Figure 2: Al2024 printed without RAM additions showing grain boundary cracking. 40X magnification

Utilizing the RAM process, Al2024 metal matrix composite specimens with 10 vol% ceramic material were additively manufactured by L-PBF using a commercial EOS M290 system. Tensile testing demonstrated high yield and ultimate tensile strength. The fracture surface, shown in Figure 3, did not show the intergranular fracture seen in the specimens produced without RAM additions. The resulting MMC had a bimodal ceramic distribution with sub-micron particles approximately 200-800 nm and larger particles approximately 5 to 20 µm and were evenly distributed throughout the material as shown by the microstructure in Figure 4. The ceramic particles acted as nucleants during solidification of the aluminum alloy resulting in fine equiaxed grains. The resulting specimens were free of microcracking and exhibited excellent tensile strength. The equiaxed grains are uncommon in fusion based AM processes and resulted in relatively isotropic mechanical properties.

Using the RAM process on an EOS M290 AM system to produce 2 vol% ceramic specimens of aluminum alloys including 2024 and 6061 resulted in highly printable materials with properties comparable to their wrought counterparts. The resultant alloys were heat treatable using the same heat treatments as the wrought alloys and exhibited comparable mechanical properties. Increased ceramic volume fractions increased yield strength, ultimate tensile strength, and hardness but decreased elongation as shown in Tables I and II. These tables also show the respective wrought alloy properties for comparison to the additively produced versions.

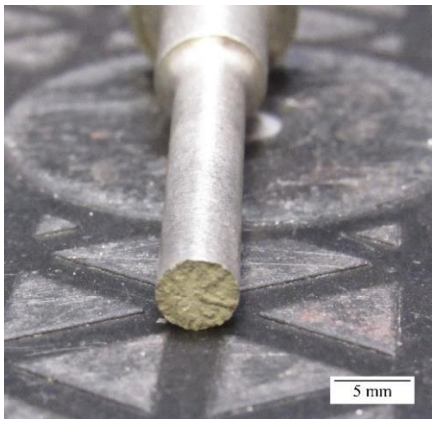

Figure 3: Macroscopic image of A2024-RAM10 tensile specimen.

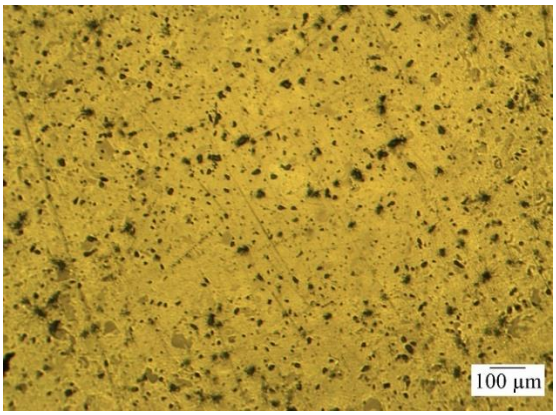

Figure 4: Image of A2024-RAM10 showing an even dispersion of ceramic particles and free of the microcracking seen in Figure 2 3. Taken at 40X magnification

Table I: Properties for wrought Al2024-T4 and additively manufactured Al2024-RAM alloys.

Properties	Wrought Al2024-T4 [9]	A2024-RAM2	A2024-RAM10
Density (g/cm^3)	2.78	2.82	2.97
Hardness (HRB)	75	82±3	92±3
Yield Strength (MPa)	324	400	535
Tensile Strength (MPa)	469	496	555
Elongation (%)	20	10	2
Modulus of Elasticity (GPa)	73.1	79	98

Table II: Properties for wrought Al6061 and additively manufactured A6061-RAM2 alloy.

Properties	Wrought Al6061-T6 [10]	A6061-RAM2	A6061-RAM10
Density (g/cm^3)	2.7	2.73	2.898
Hardness (HRB)	60	52.8±4	66.7±3
Yield Strength (MPa)	276	285	308
Tensile Strength (MPa)	310	315	421
Elongation (%)	17	13	6
Modulus of Elasticity (GPa)	68.6	76	96.8

The deposition rates of three RAM materials on an EOS M290 system are compared to EOS version 1.20 AlSi10Mg deposition in Table II. All three RAM materials print faster than AlSi10Mg while A6061-RAM 2 more than doubles this deposition rate. The increased deposition rate results in greater productivity by the machine and enables decreased part costs and increased manufacturing profitability.

Table II: Material deposition rates on an EOS M290 AM system.

AM aluminum alloys	Deposition Rate (mm^{3}s^{-1})
AlSi10Mg	5.1
A6061-RAM 2	10.4
A2024-RAM 2	7.8
A2024-RAM 10	7.12

A tensile specimen of A6061-RAM2 is pictured in the sequence in Figure 7. The sequence depicts three different stages of a tensile test: a. pre-strained, b. necking, and c. post-fracture. Figure 7b. shows the tensile bar at 16% elongation, prior to fracture. Figure 7c. shows a typical ductile fracture geometry.

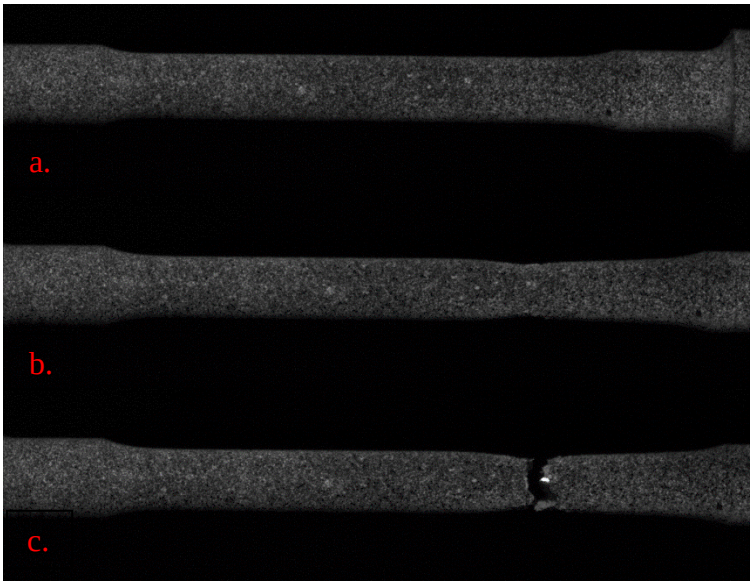

Figure 5: A6061-RAM2 tensile test images showing; a. specimen pre-strain, b. specimen at 16% elongation before fracture, exhibiting necking, c. specimen showing ductile fracture with signature cup-and-cone fracture surfaces.

Application Development

The RAM process has enabled printing of complex components, as shown in Figure 6, from desirable aluminum matrix composites including 2024 and 6061 alloys. Testing of these composite materials demonstrated improvements in strength, modulus, wear resistance, elevated temperature strength, and elevated temperature fatigue resistance compared to the respective wrought matrix alloys. The additively manufactured Al2024 MMC piston head shown in Figure 6 (left) demonstrates the light weighting capabilities of AM with the improved high temperature strength, fatigue resistance, and wear resistance a RAM produced MMC. The stator vane shown in Figure 6 (right) demonstrates the complex features including blade-like edges and internal air-cooling channels possible with RAM produced MMC materials.

Using the RAM process to produce 2 vol% ceramic aluminum 6061 and 2024 has also enabled printing of these alloys with mechanical properties comparable to their wrought counterparts. Ball Aerospace components produced from Al6061-RAM 2% are shown with permission in Figures 7 and 8. Figure 7 shows an anodized Al6061-RAM 2% lattice structured mirror blank and Figure 8 shows a chromate coated Al6061-RAM 2% spacecraft bracket.

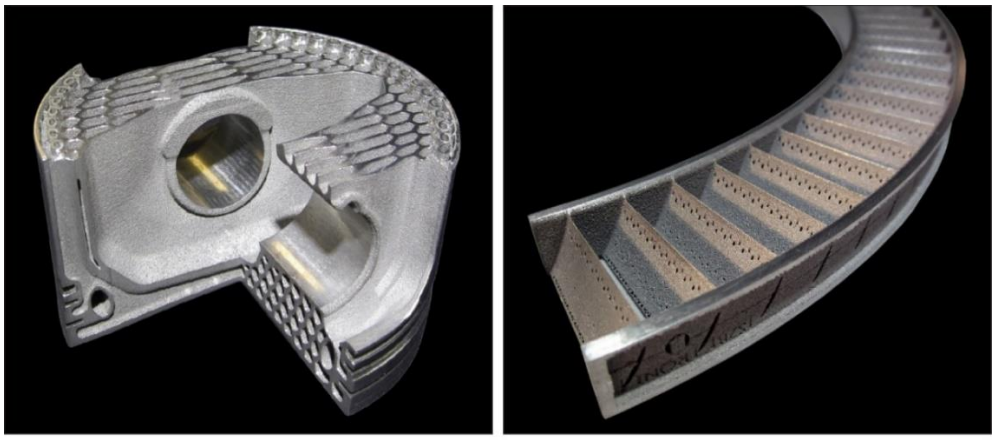

Figure 6. Aluminum piston head (left) 3D printed from a 2024 aluminum alloy developed by Elementum 3D and aluminum stator vane (right) 3D printed from a 6061-aluminum alloy developed by Elementum 3D. The parts demonstrate the printability of 2000 series and 6000 series aluminum alloys for complex parts with internal cooling channels and no evidence of cracking.

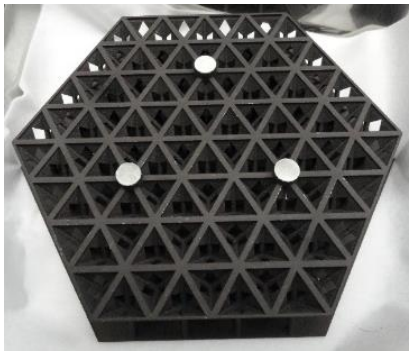

Figure 6: Additively manufactured mirror blank. Courtesy of Ball Aerospace.

Figure 7: Additively manufactured spacecraft bracket. Courtesy of Ball Aerospace.